Hindawi
International Journal of Photoenergy
Volume 2021, Article ID 2870386, 12 pages
https://doi.org/10.1155/2021/2870386

Research Article

Comprehensive Methodology to Evaluate Parasitic Energy Consumption for Different Types of Dual-Axis Sun Tracking Systems

Ming-Hui Tan,[1] **Tze-Koon Wang**,[2] **Chee-Woon Wong**,[2] **Kok-Keong Chong**,[2] **Boon-Han Lim**,[2] **Tiong-Keat Yew**,[1] **Woei-Chong Tan**,[3] **and An-Chow Lai**[2]

[1]*Faculty of Engineering and Green Technology, Universiti Tunku Abdul Rahman, Jalan Universiti Bandar Barat, 31900 Kampar, Malaysia*
[2]*Lee Kong Chian Faculty of Engineering and Science, Universiti Tunku Abdul Rahman, Bandar Sungai Long, 43000 Kajang, Selangor, Malaysia*
[3]*Faculty of Engineering and Technology, Kolej Universiti Tunku Abdul Rahman, Jalan Genting Kelang, 53300 Kuala Lumpur, Malaysia*

Correspondence should be addressed to Kok-Keong Chong; chongkk@utar.edu.my

Received 5 June 2021; Revised 15 August 2021; Accepted 2 November 2021; Published 20 November 2021

Academic Editor: Koray Ulgen

A dual-axis sun tracking system is an essential strategy to maximize the optical efficiency of harnessing solar energy. However, there is no significant study yet to optimize the net performance of the photovoltaic (PV) or concentrator photovoltaic (CPV) system equipped with a dual-axis sun tracking system. Parasitic energy loss associated with the power consumption of the sun tracking system is one of the major concerns for the solar industrial players. To address this issue, a comprehensive methodology has been developed to evaluate the yearly cumulative range of motion for dual-axis sun tracking systems in the cases of with and without fixed parking positions across the latitudes ranging from 45°N to 45°S. The parasitic energy consumptions have been investigated for three selected types of dual-axis sun tracking systems, i.e., the azimuth-elevation sun tracking system (AE-STS), polar dual-axis sun tracking system (PD-STS), and horizontal dual-axis sun tracking system (HD-STS). The simulated results indicate that the dual-axis sun tracking system with the nonfixed parking (or stow) position has lower yearly cumulative parasitic energy consumption with respect to the sun tracking system with a fixed parking position. Lastly, our simulation result has shown that the parasitic energy consumption of the sun tracking is relatively smaller to that of the electrical energy generated by the concentrator photovoltaic system with the ratio between 0.15% and 0.29% for AE-STS, between 0.15% and 0.30% for PD-STS, and between 0.17% and 0.35% for HD-STS.

1. Introduction

The awareness towards deployment of clean energy sources has recently been increasing attributed to the extreme floods and droughts that resulted from global warming. As the most abundant natural resource, the energy irradiated from the sun is clean, renewable, and ever ready to be converted into electrical energy by the means of either photovoltaic (PV) system or concentrator photovoltaic (CPV) system [1]. With the current fast progressing research and development in the solar cell materials, the power conversion efficiency of the photovoltaic system has continuously been enhancing, which has propagated strong interests among industrial players and consumers in the solar power system [2, 3]. As the sun position relative to the earth is changing throughout the day for the entire year, a sun tracking system can be integrated into the PV or CPV system to maximize the yield of solar power generation. From the past few decades, many research works have been conducted on sun tracking systems using various approaches to increase the optical efficiency and hence to improve the overall performance of the PV and CPV systems. There are two common methods to track the sun position:

single-axis and dual-axis sun tracking systems associated to the solar collectors.

For the single-axis sun tracking system, the solar collector only tracks the sun position in one-degree-of-freedom, which is less complicated in the drive mechanism. The ordinary types of single-axis sun tracking systems are the horizontal single-axis tracker (HSAT), vertical single-axis tracker (VSAT), tilted single-axis tracker (TSAT) etc. [4]. Al-Mohamad integrated the programmable logic controlling (PLC) unit into a single-axis sun tracking system to achieve an average overall performance improvement of more than 20% throughout the day in respect to that of fixed-mounted PV modules [5]. Lazaroiu et al. made a comparison of daily energy production between fixed and single-axis sun tracking PV systems by considering energy consumption of the sun tracker, and their experimental results highlighted that the sun tracker can contribute significant power generation during the morning and evening [6]. Moreover, some researchers have proposed and performed investigation on the performance of noncontinuous single-axis sun tracking PV systems [7–9]. The 1-axis-3-position (1A-3P) sun tracking PV has increased the total long-term electricity gain by 37.5% relative to that of an optimally oriented fixed PV system [7]. Gutiérrez and Rodrigo carried out energetic analyses of a simplified 2-position and 3-position north-south horizontal single-axis sun tracker. They concluded that the annual solar irradiation gains received for 2-position and 3-position single-axis trackers as compared to the equator-pointed optimally tilted fixed system ranged from 6% to 27% and 10% to 31%, respectively [9].

For the dual-axis sun tracking system, the solar collector tracks the sun position in two-degree-of-freedom to ensure that the PV modules are always normal to the solar irradiance and to eliminate the cosine loss. The most common configuration of a dual-axis sun tracking system is the azimuth-elevation sun tracking system (AE-STS). Inspired by the standard optical mirror mount, AE-STS is the most trivial design and widely deployed sun tracking approach [10]. For AE-STS, the solar collector can be freely maneuvered to rotate about two perpendicular axes: the first axis is the zenith axis (perpendicular to the ground) and the second axis is the horizontal axis (parallel with the ground). During operation, the azimuth angle and elevation angle are the sun tracking angles rotating about the zenith axis and horizontal axis, respectively, in order to align the solar collector facing towards the sun [11]. Tarabsheh et al. found that the dual-axis PV system can improve the electricity yield by 30.82% as compared to that of the fixed PV system, which offers cost saving to the PV system by reducing the module area [12]. Abdallah investigated the electricity generation by various types of PV systems in which the dual-axis tracking PV system has gained up to 43.87% of electrical output as compared to that of the fixed-mounted PV system inclined 32° to the south [13]. Based on real performance data from the PV systems installed in Spain, Gómez-Gil et al. discovered that the single-axis and dual-axis tracking flat plate systems generate 22.3% and 25.2% more annual electricity, respectively, than the fixed flat plate system [14]. From the latest studies of the dual-axis sun tracking system, the research focuses more on new strategy to improve the accuracy of the sun tracking system and optical efficiency of the solar collector. Jamroen et al. proposed the utilization of the ultraviolet sensor-based dual-axis solar tracking system to improve energy generation by 19.97% and 11.00% as compared to the fixed flat-plate system and LDR-based solar tracking system, respectively [15]. Ahmed et al. demonstrated a computer vision- and photosensor-based two-axis solar tracking system to achieve good performance in which the real-time image processing was performed by using Raspberry Pi 4 controller [16]. Yan et al. studied the effect of tracking error of the azimuth-elevation tracking device on the optical performance of the solar dish concentrator [17]. Ontiveros et al. proposed the design and evaluation of two controllers for a two-axis solar tracker with the fuzzy logic control approach, which maintains the power that is produced by photovoltaic modules at their nominal value [18].

From the aforementioned studies, it can be concluded that PV system with a sun tracking mechanism shows a significant improvement in terms of the annual electricity yield with respect to that of the fixed-mounted PV system. Nevertheless, there is inevitable parasitic energy losses in the driving mechanism of the sun tracking system, which will reduce the net output power produced by the PV system. Inspired by our previous work to study the range of motion in the heliostat field, a comprehensive study is proposed to investigate the range of motion for the on-axis sun tracking system that has much greater applications especially in both PV and CPV systems for maximizing the clean energy harnessing from the sun [19, 20]. To date, there is no study on optimizing the net performance of PV and CPV systems equipped with different dual-axis sun tracking mechanisms. In fact, the sun tracking system is well known for its effectiveness to increase the annual electricity yield of PV and CPV systems. Inevitable parasitic energy loss associated with the driving mechanism of the sun tracking system is one of the major concerns for the industries. To address this issue, it is necessary to evaluate the yearly cumulative range of motion (ROM) for the dual-axis sun tracking system across various latitudes. One of the significant contributions made by this article is the development of a comprehensive methodology to compute the yearly cumulative ROM of dual-axis sun tracking systems for the analyses of both the yearly accumulated tracking angles as well as yearly parasitic energy loss. Instead of emphasizing on the common AE-STS as conducted by most of the previous literature studies, our study embraces three selected types of sun tracking mechanisms including the AE-STS, polar dual-axis sun tracking system (PD-STS), and horizontal dual-axis sun tracking system (HD-STS).

2. Methodology

2.1. Three Types of Dual-Axis Sun Tracking System. To study the range of motion (ROM) for three selected types of dual-axis sun tracking systems, the formulas of dual-axis sun tracking angles for different types of sun trackers must be identified. In this paper, three types of dual-axis sun tracking systems as depicted in Figure 1, i.e., AE-STS, PD-STS, and HD-STS, have been studied by computing the cumulative tracking angles. Each of the dual-axis sun tracking systems has its unique mechanical configuration, which can be represented by the three orientation angles (also known as presetting parameters). In this study, the sun tracking formulas of any configuration can be derived by substituting their respective presetting parameters into the general sun tracking formula derived by Chong and Wong [10]. The primary (α) and secondary (β) angles can be listed as follows [10]:

$$\begin{aligned}
\alpha &= \arcsin\left[\cos\delta\cos\omega(\cos\zeta\cos\lambda\cos\Phi - \cos\zeta\sin\lambda\sin\phi\sin\Phi - \sin\zeta\cos\phi\sin\Phi) - \cos\delta\sin\omega(\sin\zeta\sin\phi - \cos\zeta\sin\lambda\cos\phi) + \sin\delta(\cos\zeta\cos\lambda\sin\Phi + \cos\zeta\sin\lambda\sin\phi\cos\Phi + \sin\zeta\cos\phi\cos\Phi)\right],\\
\sin\beta &= \frac{\left[\cos\delta\cos\omega(\sin\lambda\cos\Phi + \cos\lambda\sin\phi\sin\Phi) - \cos\delta\sin\omega\cos\lambda\cos\phi + \sin\delta(\sin\lambda\sin\Phi - \cos\lambda\sin\phi\cos\Phi)\right]}{\cos\alpha},\\
\cos\beta &= \frac{\left[\cos\delta\cos\omega(-\sin\zeta\cos\lambda\cos\Phi + \sin\zeta\sin\lambda\sin\phi\sin\Phi - \cos\zeta\cos\phi\sin\Phi) - \cos\delta\sin\omega(\sin\zeta\sin\lambda\cos\phi + \cos\zeta\sin\phi) + \sin\delta(-\sin\zeta\cos\lambda\sin\Phi - \sin\zeta\sin\lambda\sin\phi\cos\Phi + \cos\zeta\cos\phi\cos\Phi)\right]}{\cos\alpha}.
\end{aligned} \tag{1}$$

In the case of $\cos\ \beta \geq 0$,

$$\beta = \arcsin\left[\frac{\cos\delta\cos\omega(\sin\lambda\cos\Phi + \cos\lambda\sin\varphi\sin\Phi) - \cos\delta\sin\omega\cos\lambda\cos\varphi + \sin\delta(\sin\lambda\sin\Phi - \cos\lambda\sin\varphi\cos\Phi)}{\cos\alpha}\right]. \tag{2}$$

In the case of $\cos\ \beta < 0$,

$$\beta = \pi - \arcsin\left[\frac{\cos\delta\cos\omega(\sin\lambda\cos\Phi + \cos\lambda\sin\varphi\sin\Phi) - \cos\delta\sin\omega\cos\lambda\cos\varphi + \sin\delta(\sin\lambda\sin\Phi - \cos\lambda\sin\varphi\cos\Phi)}{\cos\alpha}\right]. \tag{3}$$

For the case of AE-STS, the two tracking angles can be obtained by substituting the presetting parameters $\phi = 0$, $\lambda = 0$, and $\xi = 0$ into the general formula as expressed in the following:

$$\alpha = \sin^{-1}(\sin\delta\sin\Phi + \cos\delta\cos\omega\cos\Phi). \tag{4}$$

In the case of $\cos\ \beta \geq 0$,

$$\beta^{+} = \sin^{-1}\left[-\frac{\cos\delta\sin\omega}{\cos\alpha}\right]. \tag{5}$$

In the case of $\cos\ \beta < 0$,

$$\beta^{-} = \pi - \beta^{+}. \tag{6}$$

For the case of PD-STS, the two tracking angles can be obtained by substituting the presetting parameters: $\phi = 180$, $\lambda = 0$, and $\xi = \Phi - 90$ into the general formula as follows:

$$\begin{aligned}
\alpha &= \delta,\\
\beta &= \omega,
\end{aligned} \tag{7}$$

when $-\pi/2 < \omega < \pi/2$.

For the case of HD-STS, the two sun tracking angles can be attained by substituting the presetting parameters as $\phi = 180$, $\lambda = 0$, and $\xi = -90$ into the general formula, as follows:

$$\begin{aligned}
\alpha &= \sin^{-1}[\sin\delta\cos\Phi - \sin\Phi\cos\delta\cos\omega],\\
\beta &= \sin^{-1}\left[\frac{\cos\delta\sin\omega}{\cos\alpha}\right].
\end{aligned} \tag{8}$$

2.2. Stow or Parking Positions for the Dual-Axis Sun Tracking System. In the simulation algorithm, stow or parking positions of solar collectors are classified under two different circumstances, which are fixed and nonfixed parking (stow) positions. The parking position refers to the inactivated position of the solar collector when the sun tracking system is not in operation especially during the period from sunset to sunrise. In practice, the solar collector of a dual-axis sun tracking system is usually oriented in such a way that it faces toward the zenith direction to minimize the wind load acting on the solar collector and such a parking position is defined as a fixed parking position. For the nonfixed parking position, it is defined as the final position of the solar collector attached to the dual-axis sun tracking system where it is halted at the end of daily operation and it normally faces toward the direction of the sunset.

2.3. Yearly Cumulative Range of Motion. To compare the ROM for different configurations, the yearly cumulative tracking angles for the three types of dual-axis sun tracking systems have been computed. The yearly cumulative ROM is defined as the summation of angular movement of the dual-axis sun tracking system during the daily operational period throughout the entire year. For the fixed parking

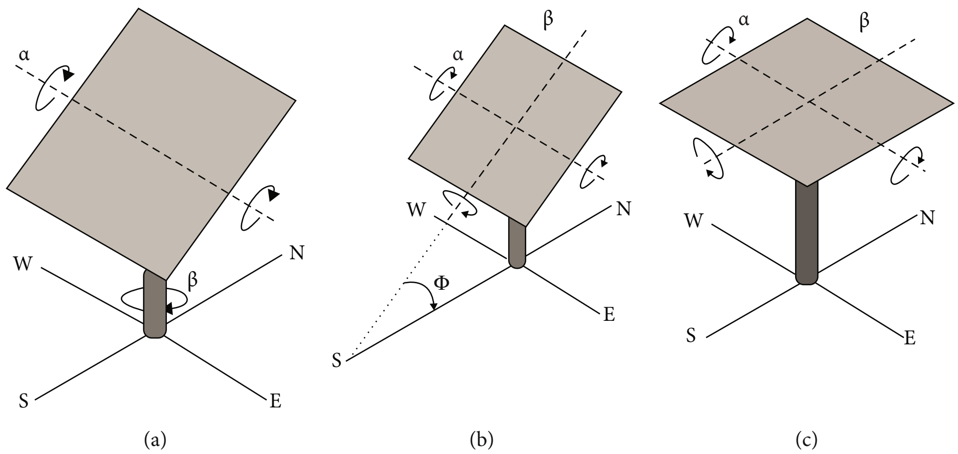

Figure 1: Three different types of dual-axis sun tracking methods: (a) azimuth-elevation sun tracking system (AE-STS), (b) polar dual-axis sun tracking system (PD-STS), and (c) horizontal dual-axis sun tracking system (HD-STS).

position, the computation of the yearly cumulative ROM is started from the parking position where the dual-axis sun tracking system is oriented to face toward the zenith direction during the sunrise and back to the initial parking position during the sunset. For the nonfixed parking position, the computation of yearly cumulative ROM starts from the last position of the solar collector in the previous daily operation moving toward the sunrise position, and then, it ends at the last position of the daily operation during the sunset. Besides, the dual-axis sun tracking system is implemented as an open-loop control system in which the angular movement of the dual-axis sun tracking system is based on the calculated tracking angles using the general sun tracking formula. Two absolute optical encoders are integrated into the driving mechanism acting as feedback sensors for keeping the accurate position of the solar collector in check every moment during operation. Hence, the angular tracking movement of the dual-axis sun tracking system is not influenced by external factors such as wind speed and intermittent weather conditions, where these factors frequently affect the active sensors using sunlight as the feedback signal. The flowchart of the algorithms to compute the yearly cumulative range of motion for three different types of dual-axis sun tracking systems and both parking positions is depicted in Figure 2.

2.4. Yearly Parasitic Energy Consumption. As the sun position varying throughout the day for the entire year, the dual-axis sun tracking system is essential to ensure the solar collector, either the PV system or the CPV system, always facing toward the sun direction in order to achieve the optimal power generation. Nevertheless, there is an inevitable parasitic energy loss, which is associated with the electrical power consumption in the driving mechanism of the sun tracker and hence decreases the net power output of the PV system or the CPV system. Thus, it is vital to take into account the parasitic energy consumption during the design phase as it may cause overestimation of net power generation from the PV system or the CPV system in the solar power plant. The specification of the dual-axis sun tracking systems for the case of CPV application is summarized in Table 1. The yearly power consumption of the sun tracking motors can be calculated by using the following formula:

$$\sum E_{\text{motor}}(\text{kWh}) = \frac{\sum\sum\beta}{\left(n_\beta(\text{rpm})/GR_\beta\right) \times 360^\circ \times 60} \times P_\beta(\text{kW}) + \frac{\sum\sum\alpha}{\left(n_\alpha(\text{rpm})/GR_\alpha\right) \times 360^\circ \times 60} \times P_\alpha(\text{kW}), \tag{9}$$

where $\Sigma\Sigma\alpha$ is the yearly cumulative primary angle α, $\Sigma\Sigma\beta$ is the yearly cumulative secondary angle β, GR_α is the gear ratio of the primary driving mechanism, GR_β is the gear ratio of the secondary driving mechanism, n_α is the angular speed of the primary motor, n_β is the angular speed of the secondary motor, P_α is the power rating of the primary motor, and P_β is the power rating of the secondary motor.

2.5. Yearly Electrical Energy Generation. To determine the yearly electrical energy generated by a solar power plant with the dual-axis sun tracking system, the yearly solar irradiation of the selected locations has to be known. The direct normal irradiance (DNI) datasets throughout the year for various locations were obtained from the ASHRAE IWEC2 weather database [21]. The locations of these cities are graphically indicated on the map as shown in Figure 3. The designated locations and the yearly average DNI for the case study have been summarized in Table 2. The equation to compute the yearly electrical energy generation of the solar power plant with a dual-axis sun tracking system is as follows:

$$\sum E_{\text{gen}} = \sum_{i=1}^{365}\sum_{j=1}^{24}\left(\text{DNI}_{(i,j)} \times A \times \eta_{\text{op}} \times \eta_{\text{con}}\right), \tag{10}$$

where A is the area of the aperture, i is the number of days, j is the number of hours in a 24-hour format, η_{op} is the optical efficiency, and η_{con} is the electrical conversion efficiency of the CPV module.

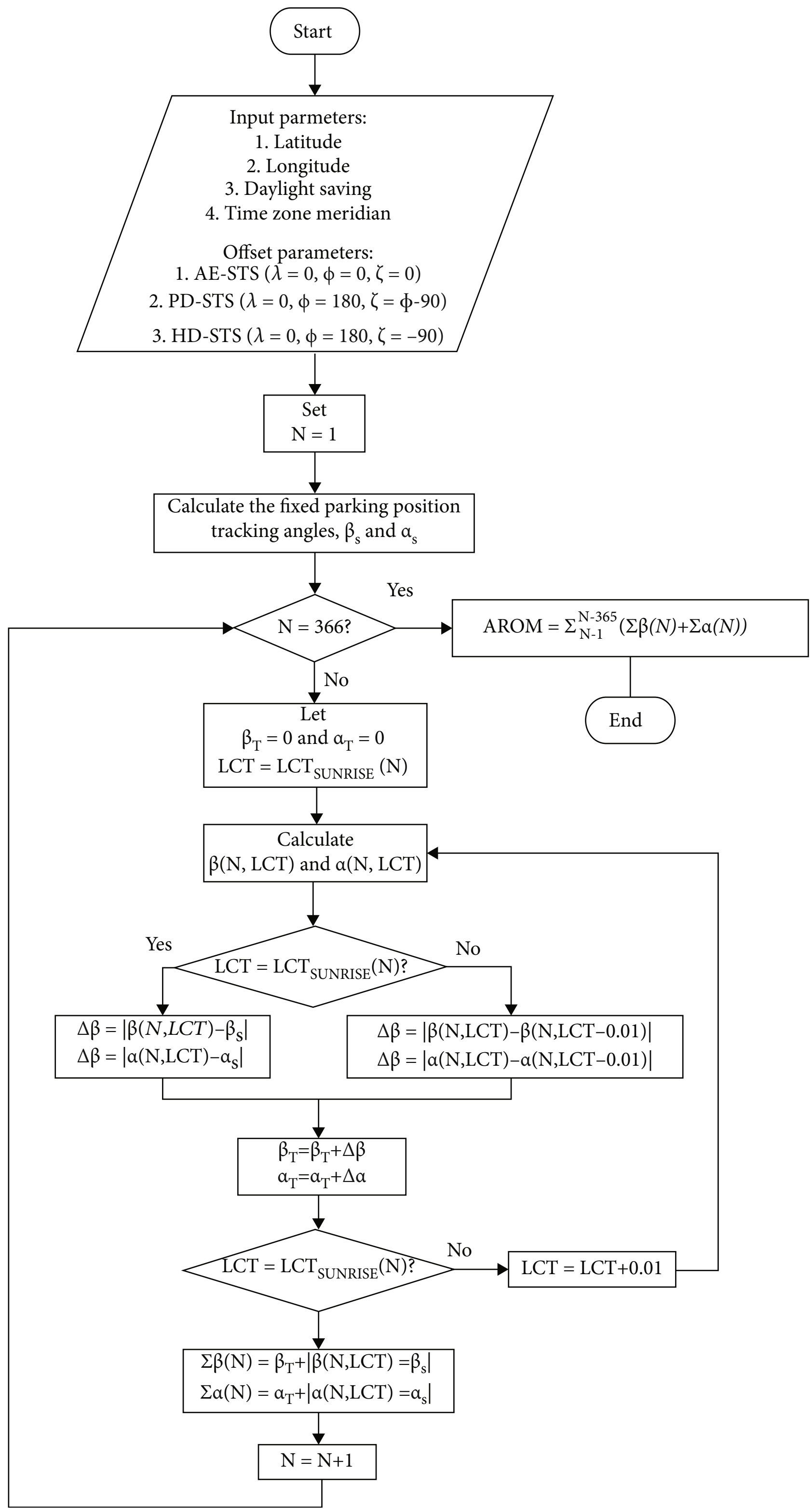

(a)

Figure 2: Continued.

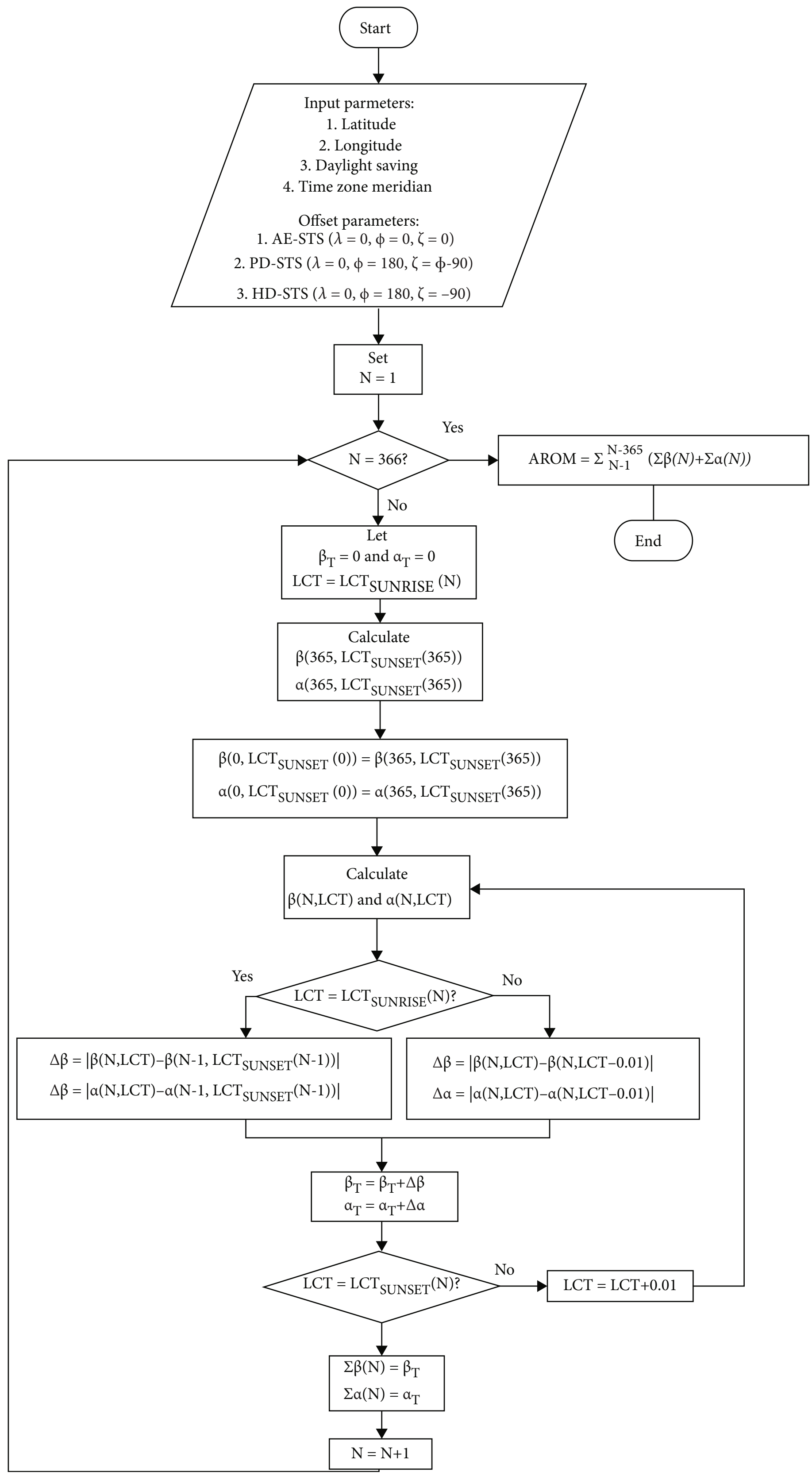

(b)

Figure 2: The flowchart to show the algorithm for calculating the yearly cumulative range of motion for different types of dual-axis sun tracking systems: (a) fixed parking position and (b) nonfixed parking position.

Table 1: Specification of the dual-axis sun tracking systems for the CPV system [3].

Description		Value	
Solar collector area, A		$25\ m^2$	
Power conversion efficiency, η_{con}		30%	
Optical efficiency, η_{op}		85%	
Angular speed of the primary motor, n_α		120 rpm	
Angular speed of the secondary motor, n_β		120 rpm	
Gear ratio of the primary driving mechanism, GR_α		4400	
Gear ratio of the secondary driving mechanism, GR_β		4400	
	AE-STS	PD-STS	HD-STS
Power rating of the primary motor, P_α	99 W	99 W	99 W
Power rating of the secondary motor, P_β	66 W*	99 W	99 W

*For AE-STS, the azimuth motor has lower power rating due to the movement not against the gravitational pull.

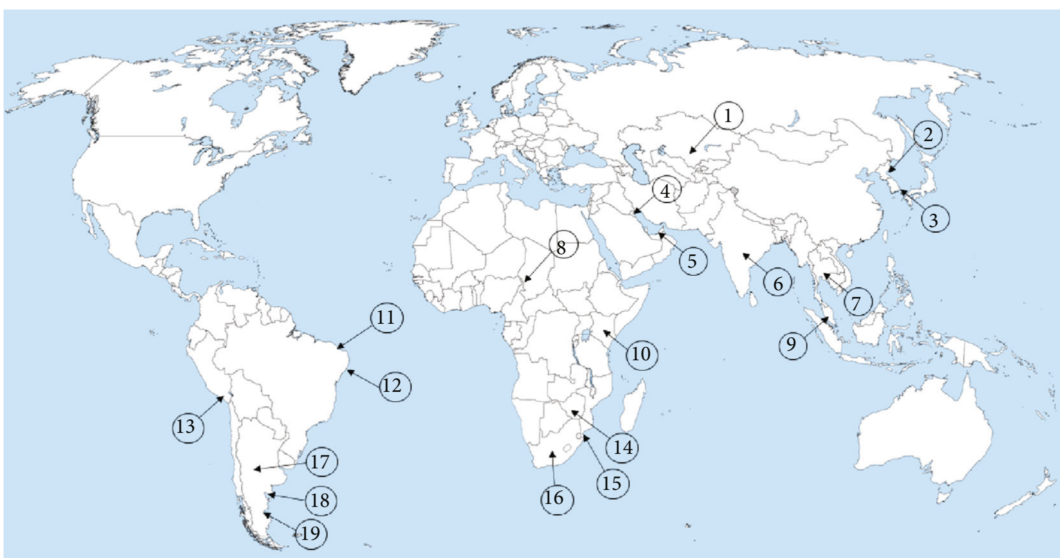

Figure 3: The location map of 19 selected cities with latitudes ranging from 45°N to 45°S for the analyses.

3. Results and Discussion

3.1. Yearly Cumulative Range of Motion. To compute the yearly cumulative ROM of the three different sun tracking systems across different latitudes ranging from 45°N to 45°S, the computational algorithm as shown in Figure 2 has been applied in our case study. The simulation of the yearly cumulative tracking angle has also been performed to calculate the yearly cumulative primary angle ($\sum\sum\alpha$) and yearly cumulative secondary angle ($\sum\sum\beta$) for three different types of dual-axis sun tracking systems with both parking positions. According to Figure 4(a), the yearly cumulative primary tracking angle is the highest while the yearly cumulative secondary tracking angle is the lowest at the equator for AE-STS. The AE-STS located proximate to both the Tropic of Cancer (23.437° N) and the Tropic of Capricorn (23.437° S) has the highest yearly cumulative secondary tracking angle for both parking positions. Moreover, the yearly cumulative primary tracking angle decreases when the latitude increases either toward the northern area or toward the southern area. The yearly cumulative primary tracking angle for AE-STS in the case of the nonfixed parking position with a reference to the fixed parking position has been reduced in the range between 54.48% and 67.12% at different latitudes, while the yearly cumulative secondary tracking angles for both fixed and nonfixed parking positions remain the same at different latitudes.

For PD-STS, the yearly cumulative secondary tracking angles for both parking positions are constant for different latitudes with the amount of 129,000° as shown in Figure 4(b). The PD-STS at the equator for the case of the fixed parking position has the lowest yearly cumulative primary tracking angle that increases proportionally with the latitude toward both northern and southern hemispheres. On the other hand, the yearly cumulative primary tracking angle of PD-STS for the case of the nonfixed parking

Table 2: Yearly average direct normal irradiance (DNI) in different cities of the world with latitudes ranging from 45°N to 45°S.

No.	City	Country	Latitude	Annual average DNI value (kWh/m^2/year)
1	Zlikha	Kazakhstan	45.3°N	1846
2	Sinpo	North Korea	40.0°N	1207
3	Busan	South Korea	35.1°N	1203
4	Kuwait City	Kuwait	29.2°N	1291
5	Abu Dhabi	United Arab Emirates	24.4°N	1269
6	Akola	India	20.7°N	1954
7	Lopburi	Thailand	14.8°N	1251
8	Ndjamena	Chad	12.1°N	1898
9	Subang	Malaysia	3.1°N	1149
10	Meru	Kenya	0.1°N	1241
11	Fortaleza	Brazil	3.8°S	1454
12	Aracaju	Brazil	11.0°S	1277
13	Arequipa	Peru	16.3°S	1964
14	Bulawayo	Zimbabwe	20.0°S	1626
15	Mavalane	Mozambique	25.9°S	1484
16	De Aar	South Africa	30.7°S	2342
17	Malargue	Argentina	35.5°S	1753
18	Viedma	Argentina	40.9°S	1752
19	Comodoro Rivadavia	Argentina	45.8°S	1300

position is constant for different latitudes with the value of 117°. The simulation result also shows that the implementation of the nonfixed parking position for PD-STS can reduce the yearly cumulative primary tracking angle by 99% relative to that of the fixed parking position in different latitudes.

In the cases of both parking positions, the result indicates that the yearly cumulative secondary tracking angle for HD-STS is constant in different latitudes with the value of 129,000°. In the cases of both parking positions, the simulation result shows that the yearly cumulative primary tracking angle for HD-STS is the lowest at the equator but it then increases proportionally with latitude toward both the northern and southern hemispheres. The result also discloses that the employment of the nonfixed parking position can reduce the yearly cumulative primary tracking angle for HD-STS by the range between 32.32% and 98.38% in respect to that of the fixed parking position.

Based on the simulated result as depicted in Figure 4, it can conclude that the implementation of the nonfixed parking position can significantly reduce the yearly cumulative primary tracking angle for all three types of dual-axis sun tracking systems in different latitudes. The yearly cumulative secondary tracking angle for both fixed and nonfixed parking positions remain the same in different latitudes.

The simulated results of total yearly cumulative ROM for the three sun tracking systems in the cases of fixed and nonfixed parking positions are illustrated in Figure 5. For the case of the fixed parking position, the total yearly cumulative ROM for all the three different sun tracking systems vary with the latitude but they are symmetrical relative to the equator ($\Phi = 0$). For the case of the nonfixed parking position, the total yearly cumulative ROM for AE-STS and HD-STS differ with the latitude but they are symmetrical relative to the equator ($\Phi = 0$). On the other hand, the total yearly cumulative ROM for PD-STS are almost constant in all latitudes in the case of the nonfixed parking position. Besides, the simulated results also show that AE-STS in the case of fixed parking position has the highest yearly cumulative ROM whilst PD-STS in the case of the nonfixed parking position has the lowest yearly cumulative ROM.

The AE-STS located proximate to the Tropic of Cancer (23.437° N) and the Tropic of Capricorn (23.437° S) has the highest yearly cumulative ROM for both parking positions. The HD-STS sited at equator ($\Phi = 0$) in both parking positions has the lowest yearly cumulative ROM while the yearly cumulative ROM starts to increase when the HD-STS is located further away from the equator toward either the north or south direction. For the case of the fixed parking position, the yearly cumulative ROM for the PD-STS has the same trend as the HD-STS. According to the simulated results, all the three different dual-axis sun tracking systems in the case of the nonfixed parking position have lower yearly cumulative ROM as compared to that of the case of the fixed parking position. This is mainly caused by all types of dual-axis sun tracking systems in the case of the nonfixed parking position having lesser yearly cumulative ROM in the secondary tracking angle. The yearly cumulative ROM for AE-STS, PD-STS, and HD-STS in the case of the nonfixed parking position with reference to the fixed parking position have been reduced in the range between 26.69% and 28.69%, 7.69% and 20.56%, and 7.38% and 8.83%, respectively. This has shown that the implementation of the nonfixed parking position can reduce the yearly cumulative ROM for three different dual-axis sun tracking systems significantly.

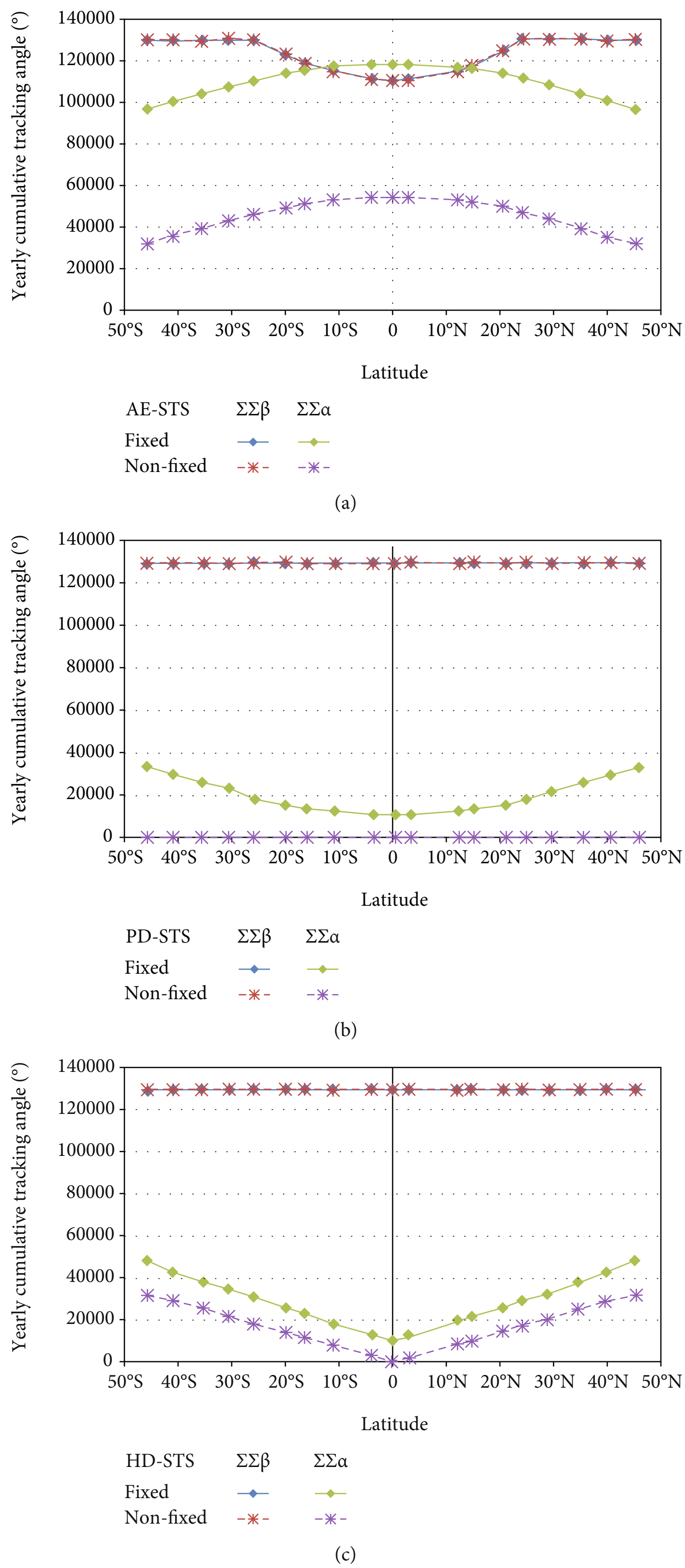

Figure 4: The yearly cumulative tracking angle of different sun tracking systems for the cases of fixed and nonfixed parking positions in various locations with latitudes ranging from 45°N to 45°S: (a) AE-STS, (b) PD-STS, and (c) HD-STS.

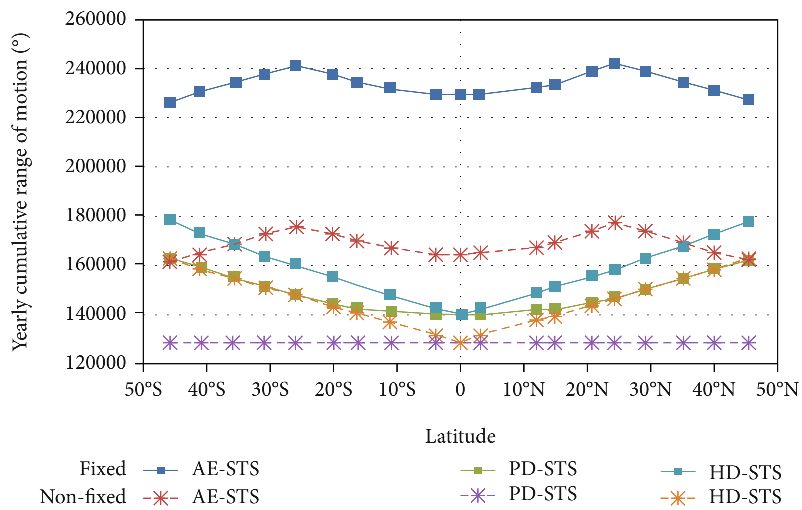

Figure 5: The yearly cumulative range of motion for three different types of sun tracking systems for the cases of the fixed and nonfixed parking positions in various locations with latitudes ranging from 45°N to 45°S.

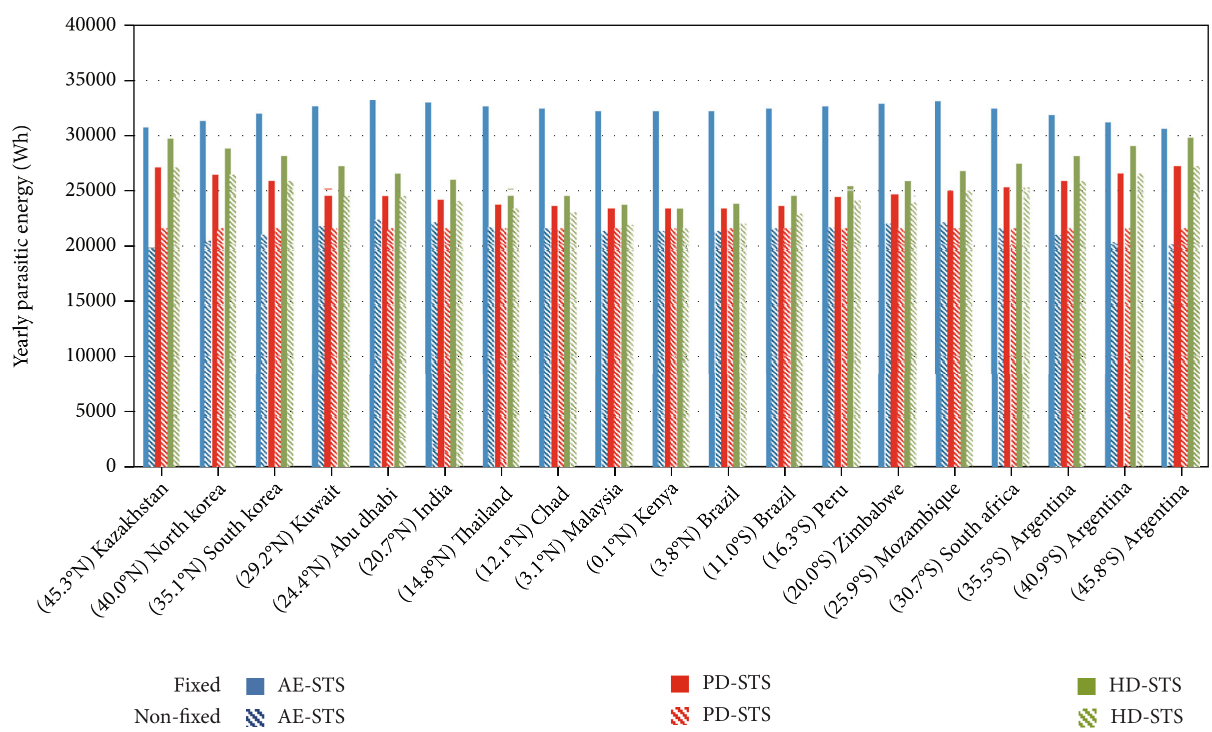

Figure 6: The yearly parasitic energy for three different sun tracking systems for the cases of fixed and nonfixed parking positions in various locations with latitudes ranging from 45°N to 45°S.

3.2. Yearly Parasitic Energy Consumption. As the inevitable parasitic energy consumed by driving mechanisms of the sun tracking system will reduce the net power generation of the PV or CPV system, it is important to study the corresponding energy consumption of the dual-axis sun tracking systems. The corresponding energy consumption of the dual-axis sun tracking systems with the specification as stated in Table 1 can be computed based on the yearly accumulated range of motion by using equation (9). Based on the simulated result as depicted in Figure 6, the yearly parasitic energy consumed by the sun tracking mechanism also varies with the latitude but they are symmetrical relative to the equator ($\Phi = 0$) for both parking positions. The AE-STS for the case of the fixed parking position has the highest yearly parasitic energy consumption among all the dual-axis sun tracking methods for all different latitudes. On the other hand, the PD-STS with the nonfixed parking position has the lowest yearly parasitic energy consumption

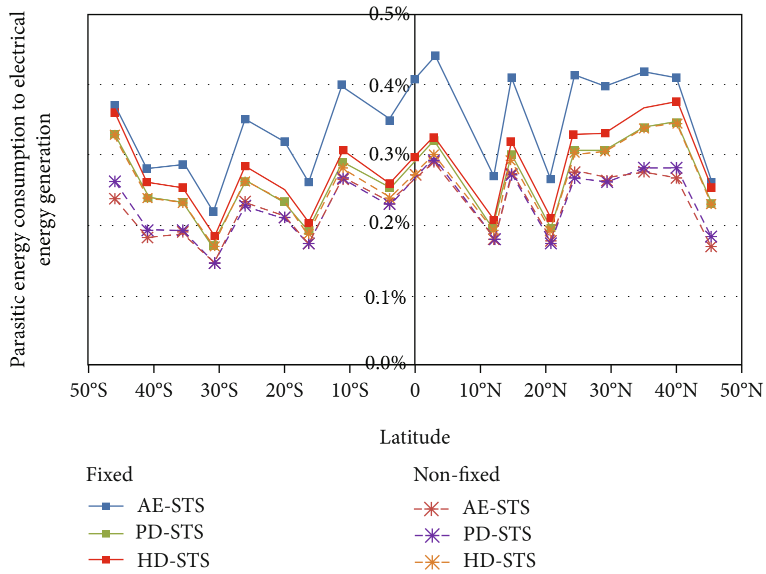

FIGURE 7: The percentage of the yearly parasitic energy consumption relative to the yearly electrical energy generation for three different types of sun tracking systems with fixed and nonfixed parking positions in various latitudes ranging from 45°N to 45°S.

whenever it is installed to operate at the region near to the Tropic of Cancer (15°N to 34°N) and the Tropic of Capricorn (15°S to 34°S). Moreover, AE-STS with the nonfixed parking position has the lowest yearly parasitic energy consumption whenever it is installed to operate at the region near the equator (14°N to 14°S), the northern region (35°N to 45°N), and the southern region (35°N to 45°N). The yearly parasitic energy consumption for AE-STS, PD-STS, and HD-STS with the nonfixed parking position relative to the fixed parking position has been reduced from 32.53% to 35.45%, from 7.68% to 20.56%, and from 7.38% to 8.83%, respectively. Therefore, it can conclude that the implementation of the nonfixed parking position can reduce the yearly parasitic energy consumption for all the three aforementioned dual-axis sun tracking systems significantly, which can improve the overall performance of the dual-axis sun tracking system. From the simulated results, PD-STS with the nonfixed parking position is preferable to install in the region near to the Tropic of Cancer and the Tropic of Capricorn while AE-DST is preferable to install in the region near to the equator and in the region of higher latitudes.

The yearly generated electricity for the dual-axis sun tracking systems has been determined via equation (10) for various locations by using local weather data and the specification as stated in Table 1. Moreover, the percentage of the yearly parasitic energy losses from the driving mechanism relative to the yearly generated electrical energy has also been evaluated. In Figure 7, the percentages of the yearly parasitic energy consumption relative to the yearly electrical energy generation for AE-STS, PD-STS, and HD-STS with the fixed parking position are in the range between 0.22% and 0.44%, between 0.17% and 0.35%, and between 0.18% and 0.38%, respectively. The result for AE-STS has a good agreement with the estimated electricity consumption calculated for an industrial large-scale dual-axis tracker [22]. Nevertheless, the percentages of the yearly parasitic energy consumption relative to the yearly electrical energy generation for AE-STS, PD-STS, and HD-STS with the nonfixed parking position are in the range between 0.15% and 0.29%, between 0.15% and 0.30%, and between 0.17% and 0.35%, respectively. The results show that the parasitic energy consumption from the driving mechanism is a small reference to the total generated electrical energy, which is favorable for improving the levelized cost of electricity (LCOE) with small investment to the sun tracking system.

4. Conclusion

In conclusion, we have analyzed the range of motion for three different types of dual-axis sun tracking systems via a comprehensive methodology developed in this article to compute the yearly cumulative range of motions. The investigation of the parasitic energy consumption in the PV or CPV system for three different types of dual-axis sun tracking systems in different latitudes has also been carried out. This methodology allows us to optimize the overall performance of the PV or CPV system by considering different options of parking positions. According to the results, the dual-axis sun tracking systems with the nonfixed parking position have lower yearly cumulative parasitic energy consumption as compared to that of the fixed parking position. The percentages of the yearly parasitic energy consumption relative to the yearly electrical energy generation for AE-STS, PD-STS, and HD-STS with the nonfixed parking position are in the range between 0.15% and 0.29%, between 0.15% and 0.30%, and between 0.17% and 0.35%, respectively. This study indicates that the parasitic energy consumption from the sun tracking mechanism is relatively small with respect to the total generated electrical energy. The study has verified that it is favorable to implement the dual-axis sun tracking system to the PV or CPV system to improve the electrical performance as the parasitic energy consumption from the driving mechanism is reasonably small.

Nomenclature

α: Primary angle
β: Secondary angle
δ: Sun declination angle
ω: Hour angle
Φ: Latitude
η_{op}: Optical efficiency
η_{con}: Electrical conversion efficiency.

Abbreviations

AE: Azimuth elevation
PD: Polar dual axis
HD: Horizontal dual axis
CPV: Concentrator photovoltaic
DNI: Direct normal irradiance
LCT: Local clock time
GR: Gear ratio
ROM: Range of motion
STS: Sun tracking system.

Data Availability

The numerical data used to support the findings of this study are included within the article.

Conflicts of Interest

The authors have no conflicts of interest to declare.

Acknowledgments

The authors would like to express their sincere gratitude to the UTAR Strategic Research Fund 2018 with project number IPSR/RMC/UTARSRF/PROJECT 2018-C1/001 (vote account 6274/011) and UTAR Research Fund 2020 Cycle 2 with project number IPSR/RMC/UTARRF/2020-C2/Y03 (vote account 6200/Y77) for the financial support.

References

[1] R. Eke and A. Senturk, "Performance comparison of a double-axis sun tracking versus fixed PV system," *Solar Energy*, vol. 86, no. 9, pp. 2665–2672, 2012.

[2] M. A. Green, E. D. Dunlop, J. Hohl-Ebinger, M. Yoshita, N. Kopidakis, and X. Hao, "Solar cell efficiency tables (version 56)," *Progress in Photovoltaics: Research Applications*, vol. 28, no. 7, pp. 629–638, 2020.

[3] M.-H. Tan and K.-K. Chong, "Influence of self-weight on electrical power conversion of dense-array concentrator photovoltaic system," *Renewable Energy*, vol. 87, pp. 445–457, 2016.

[4] K.-K. Chong and C.-W. Wong, "General Formula for on-Axis Sun-Tracking System," *Solar Collectors and Panels, Theory and Applications*, pp. 274–276, InTech Rijeka, Croatia or intechopen, 2010.

[5] A. Al-Mohamad, "Efficiency improvements of photo-voltaic panels using a sun-tracking system," *Applied Energy*, vol. 79, no. 3, pp. 345–354, 2004.

[6] G. C. Lazaroiu, M. Longo, M. Roscia, and M. Pagano, "Comparative analysis of fixed and sun tracking low power PV systems considering energy consumption," *Energy Conversion Management*, vol. 92, pp. 143–148, 2015.

[7] B. Huang, W. Ding, and Y. Huang, "Long-term field test of solar PV power generation using one-axis 3-position sun tracker," *Solar Energy*, vol. 85, no. 9, pp. 1935–1944, 2011.

[8] B. Huang and F. Sun, "Feasibility study of one axis three positions tracking solar PV with low concentration ratio reflector," *Energy Conversion Management*, vol. 48, no. 4, pp. 1273–1280, 2007.

[9] S. Gutiérrez and P. M. Rodrigo, "Energetic analysis of simplified 2-position and 3-position north-south horizontal single-axis sun tracking concepts," *Solar Energy*, vol. 157, pp. 244–250, 2017.

[10] K. Chong and C. Wong, "General formula for on-axis sun-tracking system and its application in improving tracking accuracy of solar collector," *Solar Energy*, vol. 83, no. 3, pp. 298–305, 2009.

[11] W. B. Stine and R. W. Harrigan, *Solar energy fundamentals and design*, Wiley Interscience, New York, 1985.

[12] A. Al Tarabsheh, I. Etier, and A. Nimrat, "Energy Yield of Tracking PV Systems in Jordan," *International Journal of Photoenergy*, vol. 2012, Article ID 890183, 5 pages, 2012.

[13] S. Abdallah, "The effect of using sun tracking systems on the voltage-current characteristics and power generation of flat plate photovoltaics," *Energy Conversion and Management*, vol. 45, no. 11-12, pp. 1671–1679, 2004.

[14] F. J. Gómez-Gil, X. Wang, and A. Barnett, "Energy production of photovoltaic systems: fixed, tracking, and concentrating," *Renewable Sustainable Energy Reviews*, vol. 16, no. 1, pp. 306–313, 2012.

[15] C. Jamroen, C. Fongkerd, W. Krongpha, P. Komkum, A. Pirayawaraporn, and N. Chindakham, "A novel UV sensor-based dual-axis solar tracking system: implementation and performance analysis," *Applied Energy*, vol. 299, article 117295, 2021.

[16] R. Ahmed, S. J. Oh, M. U. Mehmood et al., "Computer vision and photosensor based hybrid control strategy for a two-axis solar tracker - Daylighting application," *Solar Energy*, vol. 224, pp. 175–183, 2021.

[17] J. Yan, Z. R. Cheng, and Y. D. Peng, "Effect of tracking error of double-axis tracking device on the optical performance of solar dish concentrator," *International Journal of Photoenergy*, vol. 2018, Article ID 9046127, 13 pages, 2018.

[18] J. J. Ontiveros, C. D. Ávalos, F. Loza, N. D. Galán, and G. J. Rubio, "Evaluation and design of power controller of two-axis solar tracking by PID and FL for a photovoltaic module," *International Journal of Photoenergy*, vol. 2020, Article ID 8813732, 13 pages, 2020.

[19] K. Chong and M. Tan, "Range of motion study for two different sun-tracking methods in the application of heliostat field," *Solar Energy*, vol. 85, no. 9, pp. 1837–1850, 2011.

[20] K.-K. Chong and M. Tan, "Comparison study of two different sun-tracking methods in optical efficiency of heliostat field," *International Journal of Photoenergy*, vol. 2012, Article ID 908364, 10 pages, 2012.

[21] ASHRAE, "IWEC2 Weather Files for International Locations," http://www.equaonline.com/ice4user/indexIWEC2.html.

[22] B.-H. Lim, C. S. Lim, H. Li et al., "Industrial design and implementation of a large-scale dual-axis sun tracker with a vertical-axis-rotating-platform and multiple-row-elevation structures," *Solar Energy*, vol. 199, pp. 596–616, 2020.